Inorganic Chemistry
Article

Inorg. Chem. **2009**, *48*, 9723–9731 **9723**
DOI: 10.1021/ic9010949

Design and Synthesis of Highly Luminescent Near-Infrared-Emitting Water-Soluble CdTe/CdSe/ZnS Core/Shell/Shell Quantum Dots

Wenjin Zhang, Guanjiao Chen, Jian Wang, Bang-Ce Ye, and Xinhua Zhong*

State Key Laboratory of Bioreactor Engineering, Department of Chemistry, and School of Bioengineering, East China University of Science and Technology, Shanghai 200237, China

Received June 6, 2009

Applications of water-dispersible near-infrared (NIR)-emitting quantum dots (QDs) have been hampered by their instability and low photoluminescence (PL) efficiencies. In this paper, water-soluble highly luminescent NIR-emitting QDs were developed through constructing CdTe/CdSe/ZnS core/shell/shell nanostructure. The CdTe/CdSe type-II structure yields the QDs with NIR emission. By varying the size of CdTe cores and the thickness of the CdSe shell, the emission wavelength of the obtained nanostructure can span from 540 to 825 nm. In addition, the passivation of the ZnS shell with a substantially wide bandgap confines the excitons within the CdTe/CdSe interface and isolates them from the solution environment and consequently improves the stability of the nanostructure, especially in aqueous media. An effective shell-coating route was developed for the preparation of CdTe/CdSe core/shell nanostructures by selecting capping reagents with a strong coordinating capacity and adopting a low temperature for shell deposition. An additional ZnS shell was deposited around the outer layer of CdTe/CdSe QDs to form the core/shell/shell nanostructure through the decomposition of single molecular precursor zinc diethyldithiocarbamate in the crude CdTe/CdSe reaction solution. The water solubilization of the initially oil-soluble CdTe/CdSe/ZnS QDs was achieved through ligand replacement by 3-mercaptopropionic acid. The as-prepared water-soluble CdTe/CdSe/ZnS QDs possess PL quantum yields as high as 84% in aqueous media, which is one of the best results for the luminescent semiconductor nanocrystals.

Introduction

The successful synthesis of high-quality (narrow size distribution, high stability, and high luminescent efficiency) colloidal semiconductor nanocrystals (also referred to as quantum dots, QDs) has made QDs an attractive alternative to organic dyes in applications such as light-emitting devices, lasers, and biomedical fluorescent labels.[1−5] They present many advantages compared to organic fluorophores such as high-photoluminescence (PL) quantum yield (QY), tunable emission wavelength, multiplexing capabilities, and high photoresistance. Among all of these potential applications, biomedical labeling is currently of great interest. During the past decade, there have been many demonstrations of their use for biological imaging, ranging from single-molecule tracking to in vivo imaging and immunological labeling.[6−9] For these specific applications, nanocrystals emitting in the near-infrared (NIR) window, between 700 and 900 nm, are of particular interest. In this spectral window, the absorption by biological tissues is much more reduced compared to that in other ranges. This allows the penetration of excitation light and fluorescence photons deep into biological samples. Another advantage is the absence of autofluorescence from tissue, resulting in improved signal-to-noise ratio and sensitivity. Due to the difficulty in obtaining high-quality NIR-emitting QDs, currently, the vast majority of these

*To whom correspondence should be addressed. E-mail: zhongxh@ecust.edu.cn.

(1) Somers, R. C.; Bawendi, M. G.; Nocera, D. G. *Chem. Soc. Rev.* **2007**, *36*, 579.
(2) Burda, C.; Chen, X.; Narayanan, R.; El-Sayed, M. A. *Chem. Rev.* **2005**, *105*, 1025.
(3) Tessler, N.; Medvedev, V.; Kazes, M.; Kan, S. H.; Banin, U. *Science* **2002**, *295*, 1506.
(4) Michalet, X.; Pinaud, F. F.; Bentolila, L. A.; Tsay, J. M.; Doose, S.; Li, J. J.; Sundaresan, G.; Wu, A. M. *Science* **2005**, *307*, 538.
(5) Rogach, A. L.; Gaponik, N.; Lupton, J. M.; Bertoni, C.; Gallardo, D. E.; Dunn, S.; Pira, N. L.; Paderi, M.; Repetto, P.; Romanov, S. G.; O'Dwyer, C.; Torres, C. M. S.; Eychmuller, A. *Angew. Chem., Int. Ed.* **2008**, *47*, 6538.
(6) Dahan, M.; Levi, S.; Luccardini, C.; Rostaing, P.; Riveau, B.; Triller, A. *Science* **2003**, *302*, 442.
(7) Dubertret, B.; Skourides, P.; Norris, D. J.; Noireaux, V.; Brivanlou, A. H.; Libchaber, A. *Science* **2002**, *298*, 1759.
(8) Kim, S.; Lim, Y. T.; Soltesz, E. G.; De Grand, A. M.; Lee, J.; Nakayama, A.; Parker, J. A.; Mihaljevic, T.; Laurence, R. G.; Dor, D. M.; Cohn, L. H.; Bawendi, M. G.; Frangioni, J. V. *Nat. Biotechnol.* **2004**, *22*, 93.
(9) (a) Wu, X.; Liu, H.; Liu, J.; Haley, K. N.; Treadway, J. A.; Larson, J. P.; Ge, N.; Peale, F.; Bruchez, M. P. *Nat. Biotechnol.* **2003**, *21*, 41. (b) Kashemirov, B. A.; Bala, J. L. F.; Chen, X.; Ebetino, F. H.; Xia, Z.; Russell, R. G. G.; Coxon, F. P.; Roelofs, A. J.; Rogers, M. J.; McKenna, C. E. *Bioconjugate Chem.* **2008**, *19*, 2308. (c) Park, K.; Lee, S.; Kang, E.; Kim, K.; Choi, K.; Kwon, I. C. *Adv. Funct. Mater.* **2009**, *19*, 1553.

Published on Web 09/22/2009

biomedical labeling applications are based on II−VI materials and their corresponding type-I core/shell nanocrystals, principally CdSe and CdTe, whose emission performance is not satisfactory in the NIR window. The typical longest emission wavelength of CdSe-based QDs can only approach ~650 nm,[10] which is just below the optimal 700−900 nm NIR range for in vivo imaging. The CdTe QDs have the potential to give a NIR emission, and it has been demonstrated by a few successful examples,[11] but the emission efficiency (usually less than 10%) and stability of the QDs in this emission window are not satisfactory.

Besides the binary semiconductor nanocrystals with a narrow bulk bandgap such as InAs and CdTe, an alternative, promising route to approach NIR emission can be based on the type-II core/shell nanostructures (especially the CdTe-based ones), where both the valence and conduction bands in the core are lower (or higher) than those in the shell. Due to the spatial separation of the excitons, type-II heterostructures could give access to a longer wavelength than either the single core or shell material. Since the pioneering work by Bawendi in 2003,[12] where type-II core/shell QDs were successfully prepared using the colloidal chemical route for the first time, a series of type-II core/shell QDs such as CdTe/CdSe,[12−18] CdSe/CdTe,[19,20] CdTe/CdS,[21,22] CdS/ZnSe,[23,24] and ZnTe/CdSe[25,26] has been successively designed and prepared in very recent years, and some successful examples have been demonstrated to obtain NIR-wavelength fluorescence using the combination of two wide bandgap semiconductors to form a type-II core/shell structure. Unfortunately, synthesis of these type-II core/shell nanostructures has proven much more challenging and has not yet yielded QDs with PL QY and photoresistance comparable to their CdSe counterparts, especially for the water-dispersible ones. For example, the PL QYs reported for colloidal type-II QDs are typically low (0−10%).[12,14−18] Low QYs have been seen as an intrinsic limitation of type-II QDs. However, preparation methodologies that minimize both surface and interfacial defects may substantially improve the PL QY of type-II QDs. Accordingly, there have been several recent reports describing highly luminescent type-II core/shell QDs.[13,19,23,24] CdS/ZnSe type-II core/shell QDs with QYs up to 50%, which benefit from an intermediate ZnCdSe alloy layer with a graded composition, have been reported by Klimov and our group independently.[23,24] De Mello Donega et al. prepared anisotropic type-II CdTe/CdSe heteronanocrystals showing a remarkably high QY (up to 82%) with the use of a low temperature for shell overgrowth.[13] More recently, reports by Peng et al. presented the synthesis of CdSe/CdTe heteronanostructures emitting at 950−1000 nm with QYs up to 50%.[19] These reports clearly demonstrate that type-II core/shell nanostructures can have high PL QYs.

These potential advantages of type-II QDs mentioned above trigger us to develop an effective NIR-emitting fluorophore based on type-II QDs with high emission efficiency, high stability, and water dispersibility. The CdTe/CdSe type-II nanostructure should be the most well-studied type-II system and has been demonstrated to be convenient for tuning the emission wavelength to the NIR region. Herein, we aim to obtain the NIR emission through constructing the CdTe/CdSe type-II core/shell nanostructure. Unfortunately, the CdTe/CdSe QDs in almost all of the previous reports have very low PL QYs (usually less than 5%) in the NIR region, and no attempts of transferring theses QDs to water have been reported.[12,14−18] To obtain high PL QY for the potentially NIR-emitting CdTe/CdSe, in this work, the CdSe shell was deposited epitaxially around the CdTe core nanocrystals through the method of successive ion layer absorption and reaction (SILAR) developed by Peng et al. at a lower temperature.[27] To overcome the tendency of easy aggregation of CdTe QDs in the process of heating, capping reagents (1-tetradecylphosphonic acid and trioctylphosphine) with strong coordinating capacity to QDs and precursors were chosen. By changing the shell thickness and/or core size, through an identical procedure the emission wavelengths of the obtained core/shell nanocrystals can be tuned from the visible spectrum to near-infrared (~540−825 nm). The highest PL QY of the obtained CdTe/CdSe QDs can be up to 94%. To further improve the stability and the emission efficiency of the NIR-emitting CdTe/CdS type-II core/shell QDs in aqueous media, which is the prerequisite for the biomedical labeling application, successful experience was borrowed from the well-developed type-I heterostructures based on the additional epitaxial growth of a wide bandgap material. Herein, an additional ZnS shell was epitaxially overcoated on the outer layer of the preprepared CdTe/CdSe core/shell nanocrystals to get the CdTe/CdSe/ZnS core/shell/shell heterostructure. The additional ZnS shell, with a substantially wide bandgap, serves as a type-I heterojunction with the CdSe layer (the band offsets among CdTe, CdSe, and ZnS are shown in Scheme 1),[28] thus efficiently confining

(10) (a) Zhong, X.; Feng, Y.; Zhang, Y. *J. Phys. Chem. C*. **2007**, *111*, 526. (b) Zlateva, G.; Zhelev, Z.; Bakalova, R.; Kanno, I. *Inorg. Chem*. **2007**, *46*, 6212. (c) Jian-Ping, Ge, J. P.; Xu, S.; Zhuang, J.; Wang, X.; Peng, Q.; Li, Y.-D. *Inorg. Chem*. **2006**, *45*, 4922.
(11) (a) Zou, L.; Gu, Z.; Zhang, N.; Zhang, Y.; Fang, Z.; Zhu, W.; Zhong, X. *J. Mater. Chem*. **2008**, *18*, 2807. (b) Rogach, A. L.; Franzl, T.; Klar, T. A.; Feldmann, J.; Gaponik, N.; Lesnyak, V.; Shavel, A.; Eychmuller, A.; Rakovich, Y. P.; Donegan, J. F. *J. Phys. Chem. C* **2007**, *111*, 14628. (c) Gu, Z.; Zou, L.; Fang, Z.; Zhu, W.; Zhong, X. *Nanotechnology* **2008**, *19*, 135604.
(12) Kim, S.; Fisher, B.; Eisler, H. J.; Bawendi, M. G. *J. Am. Chem. Soc*. **2003**, *125*, 11466.
(13) Chin, P. T. K.; De Mello Donega, C.; Van Bavel, S. S.; Meskers, S. C. J.; Sommerdijk, N. A. J. M.; Janssen, R. A. J. *J. Am. Chem. Soc*. **2007**, *129*, 14880.
(14) Yu, K.; Zaman, B.; Romano va, S.; Wang, D. S.; Ripmeester, J. A. *Small* **2005**, *1*, 332.
(15) Milliron, D. J.; Hughes, S. M.; Cui, Y.; Manna, L.; Li, J.; Wang, L. W.; Alivisatos, A. P. *Nature* **2004**, *430*, 190.
(16) Halpert, J. E.; Porter, V. J.; Zimmer, J. P.; Bawendi, M. G. *J. Am. Chem. Soc*. **2006**, *128*, 12590.
(17) Li, J. J.; Tsay, J. M.; Michalet, X.; Weiss, S. *Chem. Phys*. **2005**, *318*, 82.
(18) Seo, H.; Kim, S.; Kim, W. *Chem. Mater*. **2007**, *19*, 2715.
(19) (a) Blackman, B.; Battaglia, D. M.; Mishima, T. D.; Johnson, M. B.; Peng, X. *Chem. Mater*. **2007**, *19*, 3815. (b) Blackman, B.; Battaglia, D.; Peng, X. *Chem. Mater*. **2008**, *20*, 4847.
(20) Chen, C. Y.; Cheng, C. T.; Lai, C. W.; Hu, Y. H.; Chou, P. T.; Chou, Y. H.; Chiu, H. T. *Small* **2005**, *1*, 1215.
(21) Schops, O.; Thomas, N. Le.; Woggon, U.; Artemyev, M. V. *J. Phys. Chem. B* **2006**, *110*, 2074.
(22) Wang, J.; Long, Y.; Zhang, Y.; Zhong, X.; Zhu, L. *Chem. Phys. Chem*. **2009**, *10*, 680.
(23) Ivanov, S. A.; Piryatinski, A.; Nanda, J.; Tretiak, S.; Zavadil, K. R.; Wallace, W. O.; Werder, D.; Klimov, V. I. *J. Am. Chem. Soc*. **2007**, *129*, 11708.
(24) Fang, Z.; Gu, Z.; Zhu, W.; Zhong, X. *J. Nanosci. Nanotechnol*. **2009**, *9*, 5880.
(25) Chen, C. Y.; Cheng, C. T.; Yu, J. K.; Pu, S. C.; Cheng, Y. M.; Chou, P. T.; Chou, Y. H.; Chiu, H. T. *J. Phys. Chem. B*. **2004**, *108*, 10687.
(26) Xie, R.; Zhong, X.; Basche, T. *Adv. Mater*. **2005**, *17*, 2741.
(27) Li, J.; Wang, Y.; Guo, W.; Keay, J. C.; Mishima, T. D.; Johnson, M. B.; Peng, X. *J. Am. Chem. Soc*. **2003**, *125*, 12567.
(28) Wei, S. H.; Zunger, A. *Appl. Phys. Lett*. **1998**, *72*, 2011.

Scheme 1. Schematic Diagram of Bandgap and Band Offsets (in eV) for Interfaces among CdTe, CdSe, and ZnS

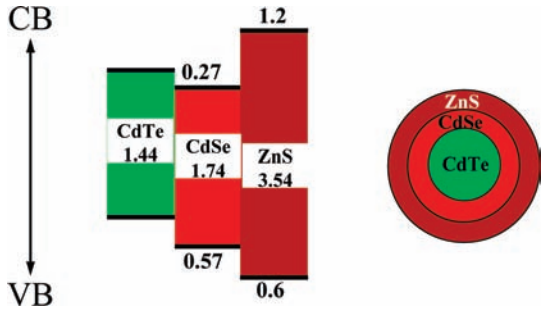

both electrons and holes within the CdTe/CdSe structure and substantially enhancing the spatial indirect radiative recombination at the CdTe core and inner CdSe shell interface. Our experimental results show that a water-dispersible, highly luminescent (with PL QY up to 86%) CdTe/CdSe/ZnS heterostructure with an emission wavelength ranging from 540 to 826 nm can be obtained conveniently. These water-dispersible, highly luminescent NIR-emitting QDs would be promising biomedical labels for ultrasensitive, multicolor, and multiplex applications, especially in the in vivo imaging applications.

Experimental Section

Chemicals. Cadmium oxide (CdO, 99.99+%), selenium powder (−100 mesh, 99.999%), tellurium powder (−200 mesh, 99.8%), 1-octadecene (ODE, 90%), trioctylphosphine (TOP, 97%), tetramethylammonium hydroxide (TMAH, 97%), and zinc diethyldithiocarbamate (ZDC, 98%) were purchased from Aldrich. Cadmium acetate hydrate ($Cd(OAc)_2 \cdot 2H_2O$, 99.99%), 3-mercaptopropionic acid (MPA, 99%), and 1-tetradecylphosphonic acid (TDPA, 98%) were purchased from Alfa. All chemicals were used as received without any further purification. All solvents were obtained from commercial sources and used as received.

Synthesis of CdTe Core Nanocrystals. CdTe core nanocrystals were prepared via a modified literature method.[29] Typically, 25.6 mg (0.2 mmol) of CdO, 140.0 mg of TDPA, and 4.0 mL of ODE were loaded in a three-neck flask clamped in a heating mantle. The mixture was heated to about 315 °C under an argon flow and resulted in a colorless clear solution, which was then cooled to 290 °C. At this temperature, 2.0 mL of the Te precursor solution (0.1 M), which was made by dissolving 127.6 mg (1 mmol) of Te in 5.0 mL of TOP at 210 °C and diluted with 5.0 mL of ODE, was quickly injected into the reaction flask. After the injection, the reaction temperature was set at 270 °C for the growth of the nanocrystals over different periods of time (30 s to 3 min) to get nanocrystals with desired sizes. The reaction mixture was then allowed to cooled to ~60 °C, and 10.0 mL of hexane/CH_3OH (v/v, 1:1) was used as the extraction solvent to separate the nanocrystals from byproducts and unreacted precursors. The as-prepared CdTe solution was further purified by centrifugation and decantation with the addition of acetone. By this approach, one can obtain CdTe QDs with an average size of 2.6−4.0 nm and a corresponding emission wavelength at λ = 560−640 nm.

Stock Solutions for CdSe and ZnS Shell Growth. The Cd precursor solution (0.1 M) was prepared by dissolving $Cd(OAc)_2 \cdot 2H_2O$ (266.5 mg) in TOP (4.0 mL) and ODE (6.0 mL) at 80 °C. The selenium precursor solution (0.1 M) was obtained by dissolving selenium (79.0 mg) in TOP (4.0 mL) and ODE (6.0 mL) using sonication. The ZnS precursor solution (0.1 M) was obtained by dissolving ZDC in TOP and ODE (v/v, 1:1) at room temperature by sonication. Each stock solution was stored at room temperature.

Synthesis of CdTe/CdSe Core/Shell and CdTe/CdSe/ZnS Core/Shell/Shell QDs. A modified SILAR technique was adopted for the growth of CdTe/CdSe core/shell nanocrystals,[27] but at a much lower temperature (150 °C) in comparison with those used in previous literature reports.[13,22] In a typical procedure, a chloroform solution of the purified CdTe QDs with emission wavelength λ = 560 nm containing 0.1 mmol of CdTe, 70 mg of TDPA, 0.5 mL of TOP, and 3.5 mL of ODE was loaded into a 50 mL flask. The flask was then pumped down at room temperature for 20 min to remove the chloroform and at 100 °C for another 20 min while flushing the reaction system twice with a flow of argon. Subsequently, the reaction mixture was further heated to 150 °C for the overgrowth of the CdSe shell. An equimolar amount of the Cd and Se precursor stock solutions was added alternately via a syringe at a 30 min interval. When the optical spectra showed no further changes, another cycle of Cd/Se precursor solution was added repeatedly. The volume of the precursor stock solution added in each cycle should not exceed the amount needed for a whole monolayer (ML) of the CdSe shell. The amount was calculated from the respective volumes of concentric spherical shells with 0.35 nm thickness for 1 ML of CdSe. With the addition of the Cd/Se precursors, the original light-red solution turned to deep red and finally to dark red gradually. To monitor the reaction, aliquots were taken before a new cycle of injection and their corresponding UV−vis and PL spectra were recorded.

In the process of overcoating the CdSe shell around the CdTe core template, when the emission wavelength of the resulting CdTe/CdSe approached the desired value, the addition of the Cd/Se precursors was stopped and the reaction temperature was lowered down to 135 °C for the following overgrowth of the ZnS shell. When the temperature of the reaction system stabilized at 135 °C, a certain amount of ZDC stock solution was added and kept at this temperature for 30 min, and then the temperature was raised to 200 °C and maintained for another 30 min. The second layer of ZnS was overcoated by repeating this heating cycle with the addition of an additional amount of ZDC stock solution. The reaction was terminated by allowing the reaction mixture to cool down to room temperature. The purification procedure was similar to that for the CdTe core nanocrystals, as mentioned above.

Water Solubilization of the Oil-Soluble QDs via Ligand Replacement. The water solubilization of the initially oil-soluble CdTe/CdSe and CdTe/CdSe/ZnS nanocrystals was achieved by replacing the initial hydrophobic surfactants (TDPA and TOP) with a hydrophilic thiol ligand (MPA) according to literature methods.[30] Typically, MPA (0.5 mL) was dissolved in 5.0 mL of methanol, and the solution was then adjusted to pH 12 with the addition of a certain amount of TMAH. The MPA−methanol solution (0.5 mL) was then added into a 5.0 mL QD chloroform solution and stirred for 30 min to get the precipitation of the QDs. Then, 5.0 mL of distilled water was added into the mixture and kept stirring for another 20 min. The solution was separated into two phases finally, and the QDs were transferred into the supernatant aqueous phase from the underlying chloroform. The underlying organic phase was discarded, and the aqueous phase containing the QDs was collected. The free MPA ligand in the QD aqueous solution was isolated by precipitating the QDs with the addition of acetone. The supernatant was discarded, and the pellet was then redissolved in water for use in the next step.

Characterization. UV−vis and PL spectra were obtained on a Shimadzu UV-2450 UV−vis spectrophotometer and a Cary

(29) Yu, W. W.; Wang, Y. A.; Peng, X. *Chem. Mater.* **2003**, *15*, 4300.

(30) Pong, B. K.; Trout, B. L.; Lee, J. Y. *Langmuir* **2008**, *24*, 5270.

Eclipse (Varian) fluorescence spectrophotometer, respectively. The room-temperature PL QYs of the QDs were determined by comparing the integrated emission of the QD samples in solution with that of a fluorescent dye (such as rhodamine 6G in ethanol (QY = 95%) or rhodamine 101 in 0.01% HCl ethanol solution (QY = 100%)) with identical optical density at the excitation wavelength.[31] Also, the known QYs of the QDs in solution can be used to measure the PL efficiencies of other QDs by comparing their integrated emission. The fluorescence lifetime study was performed using an Edinburgh FL 900 single-photon counting system equipped with a Hamamatsu C8898 ps light pulser. The excitation light was obtained from a 441 nm laser light. The luminescence time range was selected at 0−1 μs. Data were analyzed using a nonlinear least-squares fitting program, with deconvolution of the exciting pulse being ~200 ps. To conduct investigations using transmission electron microscopy (TEM), the nanocrystals were deposited from dilute solutions onto copper grids with a carbon support by slowly evaporating the solvent in the air at room temperature. TEM images were acquired using a JEOL JEM-1400 transmission electron microscope operating at an acceleration voltage of 120 kV. Powder X-ray diffraction (XRD) was obtained with wide-angle X-ray scattering, using a Siemens D5005 X-ray powder diffractometer equipped with graphite monochromatized Cu Kα radiation (λ = 1.54178 Å). XRD samples were prepared by depositing nanocrystal powder on a piece of Si(100) wafer.

Result and Discussion

Growth of CdTe/CdSe and CdTe/CdSe/ZnS Core/Shell Nanocrystals. A three-step procedure was adopted for the preparation of CdTe/CdSe/ZnS core/shell/shell nanocrystals. In the first step, CdTe nanocrystals were prepared according to the literature method developed by Peng et al. using a CdO−TDPA complex and TOPTe as the Cd and Te precursors, with the reaction carried out in a noncoordinating solvent ODE at a high temperature.[29] A CdSe shell was then overcoated around the CdTe cores by alternately adding a Cd precursor (a $Cd(OAc)_2$ solution in TOP) and a Se precursor (elemental Se solution in TOP) to a dispersion of the purified CdTe nanocrystals in a mixture solvent containing ODE, TOP, and TDPA at 150 °C according to our previous procedure for overcoating CdTe nanocrystals.[22] As mentioned in our previous report on overcoating oil-soluble CdTe QDs,[22] the purified CdTe core QDs tended feasibly to aggregate and precipitated out in the solution accompanied with rapid PL quenching in the process of heating for shell growth if the conventional reaction media composed of noncoordinating solvent ODE and primary amines were adopted. To overcome the liability of aggregation of the CdTe core, capping agents TDPA and TOP, which bear a strong coordinating capacity to cation and anion ions, respectively, were adopted in the overgrowth of the CdSe shell. Experimental results demonstrated that, with the selection of the surfactants TDPA and TOP with strong coordinating capacity, CdTe core nanocrystals can disperse well in the heating process for CdSe shell growth. The synergic effect of the selected surfactants (TDPA and TOP) with strong coordinating capacity, the appropriate reactivity of the precursors, and the low deposition temperature (150 °C) ensured that heterogeneous nucleation and growth of CdSe at the surface of the CdTe nanocrystals prevailed, and also prevented the growth of CdTe cores by Ostwald ripening or alloying due to atomic interdiffusion. High-quality CdTe/CdSe core/shell QDs with the desired shell thickness and corresponding emission wavelength can thus be obtained.

When the CdSe shell grew to the desired thickness and the corresponding PL emission wavelength of the resulting CdTe/CdSe core/shell QDs approached the desired value, a ZnS shell was consecutively epitaxially overcoated around the outer layer of the CdTe/CdSe template to form the CdTe/CdSe/ZnS core/shell/shell QDs. The selected solvent system was effective in overcoating CdSe around CdTe core nanocrystals for the formation of a CdTe/CdSe core/shell nanostructure, but it did not work in overcoating the ZnS shell around the CdTe/CdSe QDs if the conventional zinc carboxylate salts (such as zinc acetate) and elemental sulfur were adopted as the Zn and S precursors for the formation of a ZnS shell as used in the literature.[32,33] Experimental results demonstrated that, even when an excess amount of conventional Zn/S precursors was added and the growth temperature was raised to 280 °C, no observable increase of the particle size was found. The unsuccessful deposition of ZnS around the CdTe/CdSe was also confirmed by the PL quenching completely when the claimed ZnS overcoated CdTe/CdSe QDs were transferred into aqueous media. In order to overcome the difficulty of coating the ZnS shell around the CdTe/CdSe nanocrystals, we used ZDC as the single molecular precursor for the ZnS shell. The metal complexes of diethyldithiocarbamate have been well-established as the single molecular precursor for the preparation of metal sulfides nanocrystals.[34] They decomposed at an intermediate temperature to form metal sulfide nanocrystals in the presence of appropriate capping reagents. Our experimental results demonstrated that it was an efficient route to epitaxially overcoat the ZnS shell around the CdTe/CdSe nanocrystal template via the thermal decomposition of ZDC at an intermediate temperature in the crude CdTe/CdSe reaction solution. So when the CdSe shell in the CdTe/CdSe system approached the desired thickness, a certain amount of ZDC stock solution was added into the crude CdTe/CdSe reaction solution for the overgrowth of the ZnS shell around the CdTe/CdSe nanocrystals to get the CdTe/CdSe/ZnS with a desired thickness of the ZnS layer.

Figure 1 shows wide-field TEM images of CdTe core nanocrystals with an average size of 2.6 nm and the representative CdTe/CdSe and CdTe/CdSe/ZnS core/shell nanocrystals derived from the initial CdTe cores via the consecutive overgrowth of the CdSe and ZnS shells. The average sizes of the nearly dot-shaped core/shell nanocrystals (3.2, 4.0, 4.8, 5.5, and 6.7 nm corresponding to QDs containing a one-, two-, three-, and

(31) (a) Zhong, X.; Feng, Y.; Knoll, W.; Han, M. *J. Am. Chem. Soc.* **2003**, *125*, 13559. (b) Zhong, X.; Han, M.; Dong, Z.; White, T.; Knoll, W. *J. Am. Chem. Soc.* **2003**, *125*, 8589.

(32) Xie, R.; Kolb, U.; Li, J.; Basche, T.; Mews, A. *J. Am. Chem. Soc.* **2005**, *127*, 7480.

(33) Chen, Y.; Vela, J.; Htoon, H.; Casson, J. L.; Werder, D. J.; Bussian, D. A.; Klimov, V. I.; Hollingsworth, J. A. *J. Am. Chem. Soc.* **2008**, *130*, 5026.

(34) (a) Trindade, T.; O'Brein, P.; Zhang, X. *Chem. Mater.* **1997**, *9*, 523. (b) Ludolph, B.; Malik, M. A.; O'Brein, P.; Revaprasadu, N. *Chem. Commun.* **1998**, 1849. (c) Trindade, T.; O'Brien, P.; Pickett, N. L. *Chem. Mater.* **2001**, *13*, 3843. (d) Nair, P. S.; Radhakrishnan, T.; Revaprasadu, N.; Kolawole, G. A.; O'Brien, P. *Chem. Commun.* **2002**, 564.

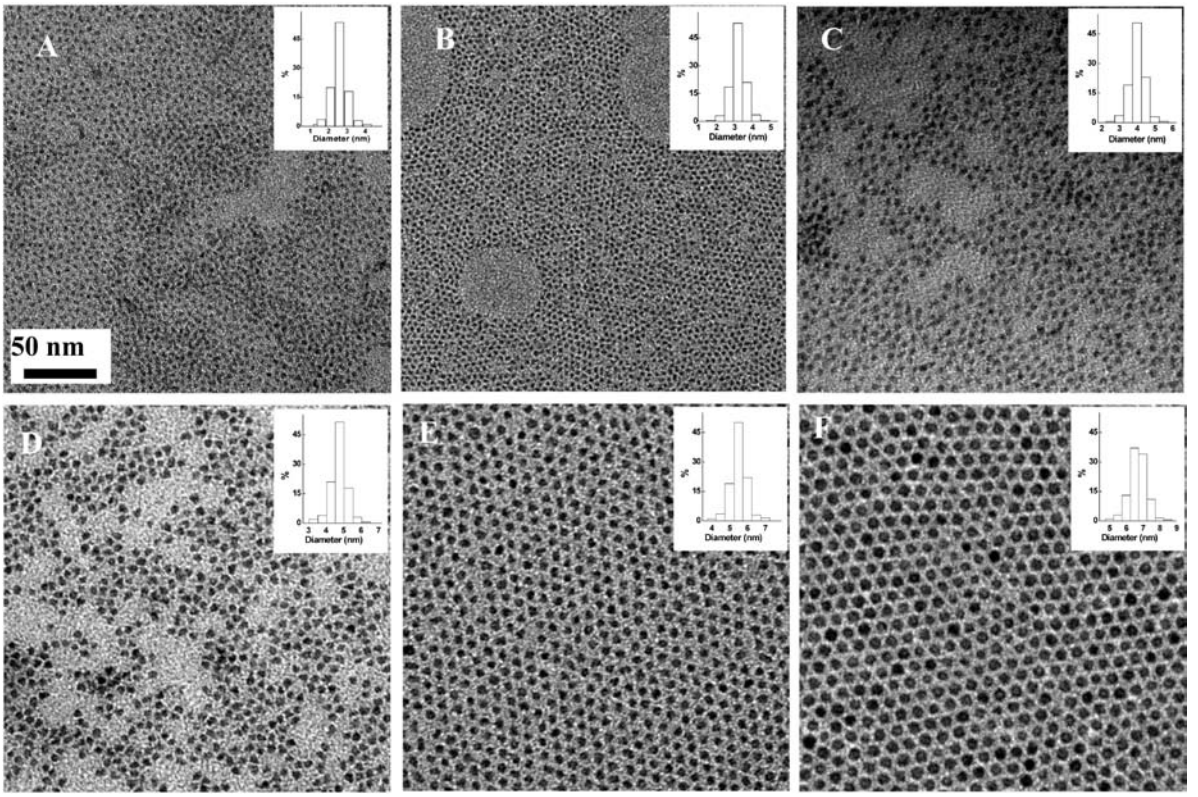

Figure 1. Wide-field TEM images of 2.6 nm CdTe core QDs (A) and the resulting CdTe/CdSe and CdTe/CdS/ZnS core/shell QDs with different shell thicknesses obtained by consecutively growing the CdSe and ZnS shells on the initial CdTe cores: (B) one-ML CdSe, (C) two-ML CdSe, (D) three-ML CdSe, (E) four-ML CdSe, (F) four-ML CdSe + two-ML ZnS. The scale bar is the same for all images. Insets are the corresponding histograms of the size distribution.

four-ML CdSe shell and a four-ML CdSe + two-ML ZnS shell, respectively) in Figure 1 approximately match the theoretical thickness calculated from the amount of injected stock solution, which gives strong evidence for the epitaxial growth of CdSe onto the CdTe cores and the overgrowth of ZnS around the CdTe/CdSe and excludes the independent homogeneous nucleation of CdSe and ZnS. All of the samples of the as-prepared CdTe/CdSe and CdTe/CdSe/ZnS core/shell nanocrystals have a narrow size distribution with a relative standard deviation (σ) of 6−8% without any postpreparation fractionation or size sorting, and the corresponding histograms of the size distribution are given in insets of Figure 1. It should be noted that the morphologies of our obtained CdTe/CdSe and CdTe/CdSe/ZnS are dot-shaped, which is different from the anisotropic prolated to branched shape as observed in the recently reported CdTe/CdSe QDs bearing high PL QYs.[13] As reported by Peng et al., the dot-shaped heterostructures are favored for maintaining high PL QYs when transferred in aqueous media.[19]

Powder XRD patterns for CdTe cores and for representative CdTe/CdSe and CdTe/CdSe/ZnS heterostructures are presented in Figure 2. The XRD pattern of CdTe nanocrystals consists of the characteristic peaks of cubic zinc blende CdTe. The diffraction peaks are broadened due to the finite particle size. When the CdSe shell is overgrown around the cubic CdTe template, the general pattern of the cubic lattice is maintained in the core/shell structures, but the diffraction peaks shift to larger angles consistent with the smaller lattice constant for CdSe compared with CdTe. With the further overgrowth of

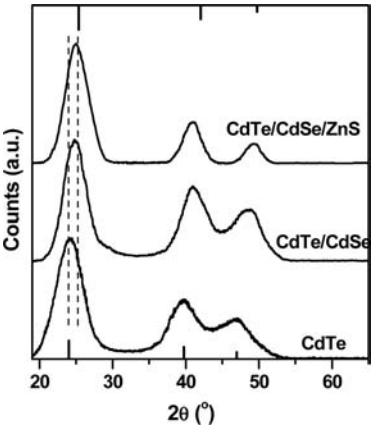

Figure 2. XRD patterns of the initial CdTe core and the resulting CdTe/CdSe core/shell QDs with a four-ML CdSe shell and CdTe/CdSe/ZnS core/shell/shell QDs with a four-ML CdSe + two-ML ZnS shell.

the ZnS shell around the outer layer of the CdTe/CdSe, the diffraction peak positions have no significant shift. In addition, the diffraction peaks narrow further with the overcoating of shell materials. This narrowing indicates that the crystalline domain is larger for the core/shell structure, providing direct evidence for epitaxial growth of the shell.

Optical Properties of CdTe/CdSe and CdTe/CdSe/ZnS Heterostructure QDs. The most direct and immediate evidence for the shell growth comes from the optical spectra. Figure 3 shows the evolution of the absorption and PL spectra of CdTe/CdSe nanocrystals. The sole PL

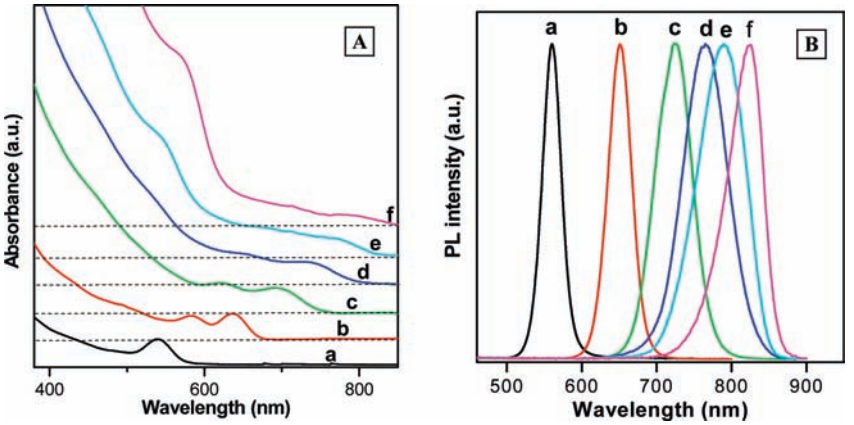

Figure 3. Normalized UV−vis spectra (A) and PL spectra (λ_{ex} = 400 nm) of CdTe cores with a diameter of 2.6 nm (a) and CdTe/CdSe core/shell QDs starting from the CdTe cores but with different MLs of CdSe shell: (b) one, (c) two, (d) three, and (e) four. For spectrum f, the CdTe core diameter is 3.0 nm and the CdSe shell thickness amounts to four MLs.

peak in the PL spectra and no corresponding CdSe absorption peaks in the absorption spectra can rule out the separate nucleation of CdSe nanocrystals, which is in agreement with the results from TEM and XRD measurements. With the increase of the CdSe shell, a systematic, dramatic red-shift was observed for both the absorption onsets and the PL peaks of the resulting CdTe/CdSe nanocrystals. This spectral evolution manifests the effect of the shell thickness. In the absorption spectra (Figure 3A), with the overgrowth of shell material CdSe around the CdTe cores, it is found that, on one hand, the spectral profiles red-shift and, on the other hand, the distinctive absorption peaks of the initial CdTe cores are eroded gradually and the excitonic absorption peak broadens and finally evolves into a featureless absorption tail when the shell thickness is up to two MLs. This observed featureless absorption tail in the absorption spectrum is characteristic of a type-II core/shell structure.[12,35] This is because of the spatial separation of the charge carried in type-II core/shell QDs and thus causes type-II core/shell QDs to effectively behave as indirect semiconductors near the band edges. Furthermore, the core/shell QDs show a remarkable increase in relative absorbance over the cores in the short wavelength region as a result of the higher effective density of states expected there due to their larger size, while on the other hand, they have relatively little absorbance near the band edge because of the weaker oscillator strength that results from the decreased wave function overlap due to the spatial separation of the charge carriers.[36] The evolution of absorption spectra clearly demonstrates a progressive reduction of the electron−hole function overlap and the formation of the indirect exciton as the dimension of the CdSe shell increased, ultimately leading to a characteristic type-II behavior. The gradual evolution of semiconductor heterostructures from type-I toward a type-II optical behavior has also been observed in CdTe/CdSe[12−18] and CdS/ZnSe[23,24] systems. This is because the energy alignment can change in the case of nanostructures, in which the alignment of quantized energy states is determined not only by bulk energy offsets but also by confinement energies determined by the heterostructure dimensions.[35a]

With the increase of the CdSe shell thickness to one, two, three, and four MLs, the corresponding PL peaks shift to λ = 652, 725, 758, and 789 nm, respectively, from the original λ = 560 nm for the CdTe cores. The PL emissions from these core/shell nanocrystals span from the visible spectral window to the NIR. It should be highlighted that the deep red to NIR window emission is of special interest for biomedical imaging because of the enhanced contrast resulting from separation of the nanocrystals' emission from the autofluorescence background and increased penetration of excitation and emission light through tissue. The emission of type-II core/shell QDs originates from the radiative recombination of electron−hole pairs across the core−shell interface. This can explain why the emission from the CdTe/CdSe core/shell is observed at wavelengths longer than the bandgap emission of either CdTe or CdSe with the same size. The PL emission of CdTe/CdSe QDs should be attributed to an excitonic transition involving the relaxed electron (mainly localized in the conduction band of the CdSe shell) and hole states (mainly localized at the valence band of the CdTe core), which is illustrated in Scheme 1. Because the energy of the valence band of the CdTe core is independent of the thickness of the CdSe shell and the energy of the conduction band of the CdSe shell is also independent of the size of the CdTe core, both the core size and the thickness of the shell can influence the effective bandgap of the core/shell structure through quantum-confinement effects. As a result, their emission wavelength can be tuned by the variation of these two variables. In other words, tuning the PL emission range is feasible by the variation of both the core size and the shell thickness. Curve f in Figure 3B shows that, when larger CdTe cores (d = 3.0 nm, emission wavelength of 610 nm) are used for the growth of CdTe/CdSe core/shell QDs, the maximum emission wavelength can be further tuned to 824 nm.

With overcoating of the CdSe shell, the QYs of the CdTe/CdSe core/shell nanocrystals increased steadily

(35) (a) Balet, L. P.; Ivanov, S. A.; Piryatinski, A.; Achermann, M.; Klimov, V. I. *Nano Lett.* **2004**, *4*, 1485. (b) Nanda, J.; Ivanov, S. A.; Htoon, H.; Bezel, I.; Piryatinski, A.; Tretiak, S.; Klimov, V. I. *J. Appl. Phys.* **2006**, *99*, 034309.

(36) Laheld, U. E. H.; Pedersen, F. B.; Hemmer, P. C. *Phys. Rev. B* **1995**, *52*, 2697.

from ~24% for the original core particles, reaching a highest value of ~94% when one ML of CdSe was fully formed and the corresponding PL emission wavelength red-shifted to 652 nm. Even though the PL QY decreased gradually when a thicker CdSe layer was overcoated around the CdTe cores, the PL QY for the CdTe/CdSe core/shell nanocrystals with four MLs of the CdSe shell corresponding to emission wavelength at 789 nm could still be kept at 46%, as shown in Figure 4. As shown in Figure 5, the obtained CdTe/CdSe QDs are very bright, even in natural room light illumination. It should be highlighted that the PL QY of 94% for the obtained CdTe/CdSe core/shell QDs is one of the best results among all of the previously reported CdTe/CdSe heteronanostructures,[12−17] which is also among the best results even in the well-developed binary II−VI semiconductor nanocrystals or their corresponding type-I heteronanostructures.[32,33,37,38] Before the pioneering work by De Mello Donega and co-workers,[13] low PL QY had been thought of as an intrinsic property of type-II heteronanostructures since the slower radiative recombination of indirect excitons should facilitate the dominance of nonradiative recombination. However, recent achievements of highly luminescent type-II heterostructures developed independently by our own group[24] and the Klimov,[23] De Mello Donega,[13] and Peng groups,[19] where CdS/ZnSe, CdTe/CdSe, and CdSe/CdTe heteronanostructures with PL QYs of more than 50% were obtained, demonstrate that low PL QYs are not intrinsic properties of the type-II heteronanostructures, and the low QYs may be due to the preparation methodologies. Through careful tailoring of the shell growth techniques that minimize both surface and interfacial defects, the PL QYs of type-II QDs may substantially improve. Here, the high PL QYs of CdTe/CdSe with a thin shell layer (less than two MLs) are due to the passivation of the core surface by the shell and thus reduce the PL quenching centers and hence improve the QY. In this case, the system behaves more like a type-I structure, where the electron−hole recombination occurs mainly in the core, as they do not show the featureless sub-band-gap absorption tail indicative of the spatially indirect transitions expected for type-II QDs. Therefore, the surface passivation plays a dominant role. These high PL QYs indicate relatively slow nonradiative recombination rates, implying low defect concentrations and therefore attesting to the high quality of the CdTe/CdSe core/shell QDs prepared in this work. The low defect concentration is probably due to the combination of slow epitaxial growth and conditions that favor effective surface passivation, relaxation, and reconstruction. Declined QYs of the thicker-shelled CdTe/CdSe QDs may originate from several mechanisms: (i) a weaker

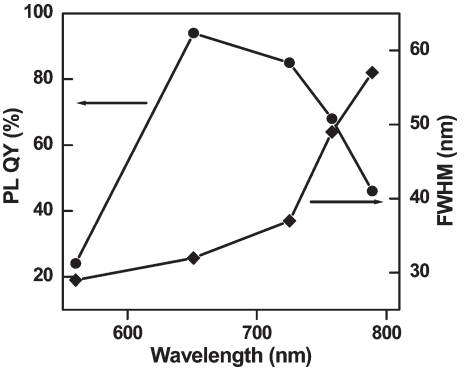

Figure 4. PL QYs and corresponding fwhm's of the obtained CdTe/CdSe core/shell QDs with different PL emission wavelengths. The emission wavelength of 560 nm corresponds to CdTe core nanocrystals.

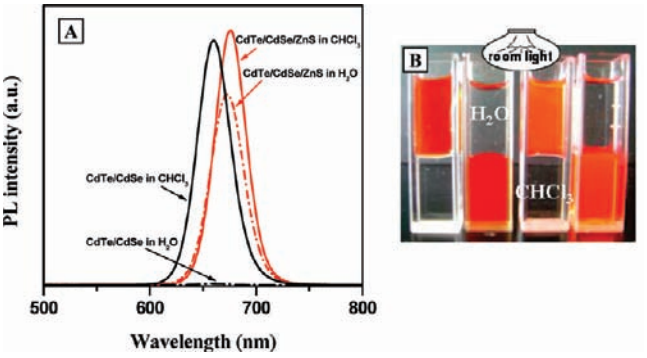

Figure 5. (A) PL spectra (λ_{ex} = 400 nm) of CdTe/CdSe (1 ML CdSe) and CdTe/CdSe/ZnS nanocrystals (1 ML CdSe, 2 ML ZnS) before (chloroform solutions) and after (aqueous solutions) phase transfer with the use of MPA. All colloidal solutions exhibit identical optical densities at the excitation wavelength. (B) Photographs of CdTe/CdSe/ZnS samples in H_2O and $CHCl_3$ under the illumination of natural room light.

quantum confinement effect due to their larger particle sizes[31a,39] and (ii) strain released through the formation of dislocations in the shell with increasing shell thickness, as observed in the well-developed CdSe/ZnS core/shell system.[38a,b] With overcoating of the CdSe shell on the CdTe cores, the full width at half-maximum (fwhm) of the resulting CdTe/CdSe core/shell nanocrystals always had at smaller values of 32−55 nm (Figure 4), which demonstrates the narrow size distribution of the obtained core/shell particles.

The high QYs of the obtained CdTe/CdSe QDs can only be retained for several days in an ambient atmosphere when dispersed in common nonpolar organic solvents. The luminescence was quenched completely if the original oil-dispersible QDs were transferred into aqueous media through ligand replacement with the use of hydrophilic thiol ligands such as MPA. Even though the construction of CdTe/CdSe type-II heterostructures yields QDs with highly luminescent NIR emission, the instability of the PL, especially in aqueous media, renders these QDs unsuitable for practical applications. The PL instability of the resulting CdTe/CdSe QDs may be due to their intrinsic band offset. From Scheme 1, we find that the electrons are localized in the outer layer of the CdSe shell. This causes the electrons to be exposed directly to

(37) (a) Talapin, D.; Rogach, A. L.; Kornowski, A.; Haase, M.; Weller, H. *Nano Lett*. **2001**, *1*, 207. (b) Donega, C. D. M.; Hickey, S. G.; Wuister, S. F.; Vanmaekelbergh, D.; Meijerink, A. *J. Phys. Chem. B* **2003**, *107*, 489. (c) Reiss, P.; Bleuse, J.; Pron, A. *Nano Lett*. **2002**, *2*, 781. (d) Foos, E. F.; Wilkinson, J.; Makinen, A. J.; Watkins, N. J.; Kafafi, Z. H.; Long, J. P. *Chem. Mater*. **2006**, *18*, 2886. (e) Qu, L.; Peng, X. *J. Am. Chem. Soc*. **2002**, *124*, 2049. (f) Peng, A.; Peng, X. *J. Am. Chem. Soc*. **2002**, *124*, 3343.

(38) Hines, M. A.; Guyot-Sionnest, P. *J. Phys. Chem*. **1996**, *100*, 468. (b) Dabbousi, B. O.; Rodriguez-Viejo, J.; Mikulec, F. V.; Heine, J. R.; Mattoussi, H.; Ober, R.; Jensen, K. F.; Bawendi, M. G. *J. Phys. Chem. B* **1997**, *101*, 9463. (c) Peng, X.; Schlamp, M. C.; Kadavanich, A. V.; Alivisatos, A. P. *J. Am. Chem. Soc*. **1997**, *119*, 7019.

(39) Norris, D.; Bawendi, M. *Phys. Rev. B* **1996**, *53*, 16338.

the solution environment and thus easily captured by the molecules in the solution system. The PL instability of the CdTe/CdSe heterostructure is similar somewhat to the case of plain CdSe QDs,[37] whose PL is also quenched completely when transferred into aqueous media due to the excitons being exposed directly to the solution environment. It has been proven that surface passivation of nanocrystals with suitable inorganic materials with a high bandgap is the key to improving PL efficiency and the stability of nanocrystals.[38] Since the pioneering work by Hines and Guyot-Sionnest,[38a] the epitaxial overgrowth of a shell of inorganic materials around CdSe core nanocrystals has been well developed, and the highly luminescent and highly stable CdSe/ZnS core/shell structures have been commercialized. On the basis of this concept, to improve the PL stability of the NIR-emitting CdTe/CdSe QDs and to make them practically applicable, several MLs of the ZnS shell were additionally epitaxially overgrown around the outer layer of the CdTe/CdSe QDs to form the CdTe/CdSe/ZnS core/shell/shell nanostructure. The additional ZnS shell, with a substantially wide bulk bandgap (E_g = 3.54 eV) compared to those of both CdTe and CdSe (E_g = 1.44 and 1.74 eV for CdTe and CdSe, respectively), serves to form a type-I heterostructure with the CdSe layer, thus efficiently confining both electrons and holes within the CdTe/CdSe structure and substantially enhancing the spatial indirect radiative recombination at the CdTe core and inner CdSe shell interface. Furthermore, the ZnS material exhibits relatively higher stability under ambient conditions in comparison with other normal high-bandgap semiconductors, which benefits surface passivation.

An additional layer of ZnS was overgrown furthermore around the CdSe layer in the original CdTe/CdSe reaction solution via the addition of the ZnS single molecular precursor ZDC. The ZnS shell deposited epitaxially around the CdTe/CdSe template with the gradual thermal decomposition of ZDC and the formation of ZnS in situ. Figure 1E shows the representative TEM image of the resulting CdTe/CdSe/ZnS core/shell/shell heterostructure with two MLs of ZnS shell consecutively overgrowing around the CdTe/CdSe core/shell nanocrystals with four MLs of CdSe shell. Upon the growth of the additional ZnS shell, no substantial change in the PL emission spectra was observed, although a slight red shift of the emission wavelength was observed (Figure 5). If compared with the original CdTe/CdSe nanocrystals, the PL QYs of the CdTe/CdSe/ZnS nanocrystals in the organic media (from 45% to 95%) improve a little bit, but increase remarkably (up to 80%) when dispersed in aqueous media via the replacement of the hydrophobic ligands by MPA. As mentioned above, the luminescence of the CdTe/CdSe QDs was quenched completely when transferred to aqueous media. For visibility, Figure 5B shows the luminescence photographs of two representative CdTe/CdSe/ZnS samples with emission wavelengths in the visible light range to demonstrate the highly bright luminescence in both oil media and aqueous media under the illumination of natural room light. The high luminescence of the CdTe/CdSe/ZnS in aqueous media can be retained for several days without observable quenching. This high PL stability of the water-soluble

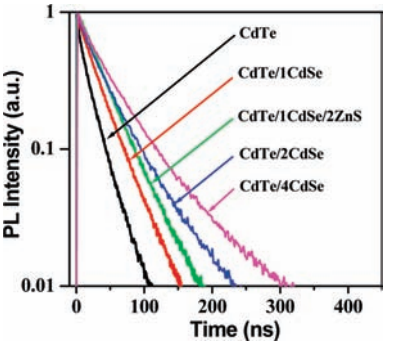

Figure 6. PL decay curves of CdTe, CdTe/CdSe, and CdTe/CdSe/ZnSe QDs with different MLs of shell material, as indicated in the legend. Emission is monitored at the exitonic peak wavelength of the corresponding QDs.

NIR-emitting QDs renders them of special interest in in vivo imaging applications.

To further investigate the difference among the plain CdTe, CdTe/CdSe, and CdTe/CdSe/ZnS heterostructures, we measured the decay curves of the exciton emission of CdTe cores and the corresponding CdTe/CdSe and CdTe/CdSe/ZnS heterostructures, which are shown in Figure 6. Herein, the room temperature PL decay time (i.e., the exciton lifetimes, $\tau_{1/e}$), at which the PL intensity has decreased to $1/e$ of its initial value, is used as a parameter to compare the lifetime. It is found that, with the deposition of the CdSe shell around the CdTe cores and the formation of a CdTe/CdSe type-II core/shell structure, the exciton lifetime increases remarkably (CdTe cores, biexponential decay, average lifetime of 14.9 ns; 28.3, 37.8, and 44.6 ns for CdTe/CdSe with a one-, two-, and four-ML shell, respectively). When one ML of CdSe is overcoated around the CdTe cores, the optical properties of the resulting CdTe/CdSe core/shell QDs behave more like a type-I structure. Meanwhile, it is found that the initial biexponential decay curve corresponding to CdTe cores shifts to a monoexponential exciton decay accompanied by an increase in the PL QY. These results show that the contribution of the nonradiative process in the exciton decay is significantly reduced after a thin shell of CdSe is overgrown. The increase in the exciton lifetime observed for CdTe/CdSe samples with one ML of the CdSe shell is partly due to the decrease of the nonradiative decay rate, since it is accompanied by a substantial increase in the PL QY (from 24% to 94%). Previous research has revealed that the probability for the carriers to be present on the surface is increased in the QD samples with higher QYs.[40] In fact, this increased probability for the carriers to be present on the surface is a direct consequence of the optimal surface condition by reason of CdSe shell growth, which efficiently removes the carrier-quenching defects from the CdTe surface. This indicates that the concentration of surface defects is reduced and that the exciton trapping at the surface defects is less efficient as a consequence of the CdSe shell overgrowth. When two MLs of the ZnS shell were further overcoated around the CdTe/CdSe QDs with one ML of CdSe, the decay curve can still be simulated with a monoexponential curve and the decay

(40) Wang, X.; Qu, L.; Zhang, J.; Peng, X.; Xiao, M. *Nano Lett.* **2003**, *3*, 1103.

time increases slightly from 28.3 to 36.4 ns. A further increase of the thickness of the CdSe shell leads to increasingly longer exciton lifetimes and a change from single-exponential to biexponential decay. The increase of exciton decay times is ascribed to the formation of a type II structure because of the spatial separation of charges in these structures.[13,41]

Conclusion

A successful approach for preparing highly luminescent water-soluble CdTe/CdSe/ZnS core/shell/shell QDs has been presented. Experimental results indicated that a synergic effect of the selected surfactants with strong coordinating capacity to precursors and nanocrystals, the lower deposition temperature, and the use of suitable precursors for shell growth played a critical role in determining the success of overgrowing shell material around the cores template and also in determining the high luminescent efficiency of the obtained heterostructure QDs. The emission wavelength from the obtained CdTe/CdSe/ZnS QDs can span from 540 to 825 nm, which is achieved through the construction of the CdTe/CdSe type-II structure. The high PL stability of the obtained CdTe/CdSe/ZnS QDs is mainly derived from the passivation effect of the outer ZnS layer with a substantially high bandgap, which effectively confines the excitons within the CdTe/CdSe interface and isolates them from the solution environment. We expect that these water-dispersible, highly luminescent NIR-emitting QDs would be promising biomedical fluorophores for ultrasensitive, multicolor, and multiplexing applications, especially in in vivo biomedical imaging applications.

Acknowledgment. We thank the National Natural Science Foundation of China (No. 20771037), the Program for New Century Excellent Talents in University of China (NCET-06-0417), Pujiang Talents Project (07pj14032), Shuguang Project (06SG33), SRFDP (20070251014), the Program for Professor of Special Appointment at Shanghai Institutions of Higher Learning, and the National Special Fund for State Key Laboratory of Bioreactor Engineering (2060204) for financial support.

(41) Hatami, F.; Grundmann, M.; Ledentsov, N. N.; Heinrichsdorff, F.; Bimberg, D.; Ruvimov, S. S.; Werner, P.; Ustinov, V. M.; Kop'ev, P. S.; Alferov, Z. I. *Phys. Rev. B* **1998**, *57*, 4635.